Extreme nickel hyperaccumulation in the vascular tracts of the tree Phyllanthus balgooyi from Borneo

Jolanta Mesjasz Przybylowicz, Wojciech Przybylowicz, Alban Barnabas, Antony van Der Ent

New Phytologist

Research

Extreme nickel hyperaccumulation in the vascular tracts of the tree *Phyllanthus balgooyi* from Borneo

Jolanta Mesjasz-Przybylowicz[1], Wojciech Przybylowicz[1,2], Alban Barnabas[1] and Antony van der Ent[3,4]

[1]iThemba LABS, National Research Foundation, PO Box 722, Somerset West 7129, South Africa; [2]Faculty of Physics & Applied Computer Science, AGH University of Science and Technology, Al. A. Mickiewicza 30, Krakow 30-059, Poland; [3]Centre for Mined Land Rehabilitation, Sustainable Minerals Institute, The University of Queensland, St Lucia, Qld 4072, Australia; [4]Université de Lorraine – INRA, Laboratoire Sols et Environnement, UMR 1120, Nancy, France

Author for correspondence:
Antony van der Ent
Tel: +61 7 334 64055
Email: a.vanderent@uq.edu.au

Received: *3 June 2015*
Accepted: *11 September 2015*

New Phytologist (2015)
doi: 10.1111/nph.13712

Key words: elemental distribution, hyperaccumulator, micro-PIXE, nuclear microprobe, phloem, *Phyllanthus balgooyi*, X-ray microanalysis.

Summary

• *Phyllanthus balgooyi* (Phyllanthaceae), one of > 20 nickel (Ni) hyperaccumulator plant species known in Sabah (Malaysia) on the island of Borneo, is remarkable because it contains > 16 wt% Ni in its phloem sap, the second highest concentration of Ni in any living material in the world (after *Pycnandra acuminata* (Sapotaceae) from New Caledonia with 25 wt% Ni in latex).

• This study focused on the tissue-level distribution of Ni and other elements in the leaves, petioles and stem of *P. balgooyi* using nuclear microprobe imaging (micro-PIXE).

• The results show that in the stems and petioles of *P. balgooyi* Ni concentrations were very high in the phloem, while in the leaves there was significant enrichment of this element in the major vascular bundles. In the leaves, cobalt (Co) was codistributed with Ni, while the distribution of manganese (Mn) was different. The highest enrichment of calcium (Ca) in the stems was in the periderm, the epidermis and subepidermis of the petiole, and in the palisade mesophyll of the leaf.

• Preferential accumulation of Ni in the vascular tracts suggests that Ni is present in a metabolically active form. The elemental distribution of *P. balgooyi* differs from those of many other Ni hyperaccumulator plant species from around the world where Ni is preferentially accumulated in leaf epidermal cells.

Introduction

Hyperaccumulators are rare plants that accumulate trace elements to extraordinarily high concentrations (> 1000 $\mu g\, g^{-1}$ nickel (Ni)) in their living biomass (Reeves, 2003; van der Ent *et al.*, 2013b). Ni hyperaccumulator plants currently number *c.* 450 different species globally, with the greatest numbers recorded from Cuba, New Caledonia and the Mediterranean region (Baker & Brooks, 1988; Reeves, 2003). Ni hyperaccumulator plants can be categorized as either obligate or facultative species, the former restricted to ultramafic soils and displaying hyperaccumulation, the latter with populations on nonultramafic and ultramafic soils but only displaying hyperaccumulation when growing on ultramafic soils (Pollard *et al.*, 2014). Some unusual facultative species have genotypes that hyperaccumulate or do not hyperaccumulate within the same populations on ultramafic soils (Mesjasz-Przybyłowicz *et al.*, 2007). Ultramafic soils are naturally enriched in Ni, and characterized by nutrient deficiencies and cation imbalances (Proctor, 2003). Ni hyperaccumulator plants have the potential to be used in phytomining, an environmentally sustainable 'green' technology to produce Ni metal (Chaney, 1983; Chaney *et al.*, 2007; van der Ent *et al.*, 2013a). In a phytomining operation, hyperaccumulator plants are grown on ultramafic soils, followed by harvesting and incineration of their biomass to generate a commercial high-grade Ni bio-ore (Brooks *et al.*, 1998, 1999; Chaney *et al.*, 2007; Harris *et al.*, 2009; van der Ent *et al.*, 2013a).

Globally, the most enigmatic Ni hyperaccumulator species is *Pycnandra acuminata* (Pierre ex Baill.) Swenson & Munzinger (formerly *Sebertia acuminata* Pierre ex Baill. Sapotaceae) (Swenson & Munzinger, 2010) from New Caledonia, a tree up to 10 m tall with a green latex containing 11.2 wt% Ni on a FW basis or 25.7 wt% on a DW basis (Jaffré *et al.*, 1976). Recently, it was discovered that the tree *Phyllanthus balgooyi* Petra Hoffm. & A.J.M.Baker (Phyllanthaceae) from Sabah (Malaysia) has 8.9 wt% Ni in phloem tissue (Baker *et al.*, 1992; Hoffmann *et al.*, 2003) and up to 16.9 wt% Ni in its phloem sap (van der Ent & Mulligan, 2015). This species was discovered to be an Ni hyperaccumulator in Palawan (Philippines) where it occurs on montane ridges as a scandent shrub (Baker *et al.*, 1992). The herbarium material was first designated *Phyllanthus 'palawanensis'* as it differed from the more common *Phyllanthus lamprophyllus*, which is distributed in Java, Borneo, Sulawesi, Philippines, Moluccas, New Guinea and Australia. Later it was described as a new species and named after the eminent botanist Max M. J. van Balgooy who first recognized this taxon

New Phytologist

(Hoffmann *et al.*, 2003). It differs from *P. lamprophyllus* in its ecology (*P. lamprophyllus* is primarily a riparian species, whereas *P. balgooyi* grows on dry ridges), the prominent leaf venation of *P. balgooyi* and its ability to hyperaccumulate Ni (Hoffmann *et al.*, 2003). Although in the Philippines *P. balgooyi* does not generally attain a height of > 1.5 m, in Sabah it grows up to 8 m tall (Hoffmann *et al.*, 2003). The *P. balgooyi* complex is taxonomically not completely understood and there may be several

Fig. 1 (a) Mature specimen of *Phyllanthus balgooyi c*. 9 m tall, with a stem of 23 cm diameter. (b) Close-up of apical shoots with leaves. (c) Excised section of phloem tissue from the main stem. (d) Glass capillary vial tube with phloem sap of *P. balgooyi* containing up to 16.9 wt% nickel.

Table 1 Elemental concentrations in bedrock and soil from the natural habitat of Bukit Hampuan, Sabah, Malaysia

	Na	Mg	Al	P	S	K	Ca	Cr	Mn	Fe	Co	Ni	Cu	Zn
Bedrock digest	wt% (DW)							μg g^{-1} (DW)						
Bedrock below plant	0.2	46	4.5	0.007	0.1	0.01	2.4	2830	5770	103 200	20	1110	35	120

	Na	Mg	Al	P	S	K	Ca	Cr	Mn	Fe	Co	Ni	Cu	Zn
Soil total concentrations	μg g^{-1} (DW)													
Mineral soil (1)	260	13 700	35 400	120	280	39	700	6520	7330	151 000	560	1620	63	93
Mineral soil (2)	310	53 200	23 200	85	200	53	5320	3170	2800	99 100	170	1860	48	66
Organic soil	230	8600	18 500	150	530	120	5530	3940	4700	79 200	340	890	32	62
Rhizosphere soil	70	8200	12 700	130	470	57	500	2920	1170	71 600	71	580	19	42

			Na	Mg	Al	P	S	K		Cr	Mn	Fe	Co	Ni	Cu	Zn
Soil DTPA-extract	pH	EC	μg g^{-1} (DW)													
Mineral soil (1)	6.4	110	22	540	11	1.1	32	77	–	0.5	390	100	16	180	1.3	3.5
Mineral soil (2)	6.4	190	4.5	510	0.8	1	7.6	33	–	< 0.01	450	28	37	290	2.9	1.7
Organic soil	6.5	510	6.7	130	9.7	0.7	5.1	20	–	0.1	270	38	68	98	0.1	1.2
Rhizosphere soil	5.1	340	20	480	148	0.6	20	59	–	0.6	280	280	19	74	1.8	1.9

The digests and extracts were analysed with ICP-AES. EC, electrical conductivity; Na, sodium; Mg, magnesium; Al, aluminium; P, phosphorus; S, sulphur; K, potassium; Ca, calcium; Cr, chromium; Mn, manganese; Fe, iron; Co, cobalt; Ni, nickel; Cu, copper; Zn, zinc. Numbers in brackets denote separate samples analysed.

Table 2 Bulk elemental concentrations in plant tissues of *Phyllanthus balgooyi* from Sabah (Malaysia)

	Na	Mg	Al	P	S	K	Ca	Cr	Mn	Fe	Co	Ni	Cu	Zn
Tissue	$\mu g\ g^{-1}$ (DW)													
Bark (1)	22	420	93	22	96	54	120	20	45	610	2.8	370	1	11
Bark (2)	18	330	49	25	110	49	100	11	45	290	5.2	360	0.8	10
Leaves (1)	441	3010	37	370	1070	1890	6810	8.1	450	52	20	4900	4.4	58
Leaves (2)	1140	2270	35	290	1010	2550	8680	19	480	39	46	7060	4.3	140
Phloem tissue	1090	600	14	140	1310	4770	3210	8.5	160	24	252	45 010	10	410
Phloem sap (1)	530	820	30	140	810	650	1300	1.4	350	15	1869	145 600	1	3690
Phloem sap (2)	430	810	25	150	920	1210	1870	2.9	480	15	1449	168 500	0.9	2380
Phloem sap (3)	930	600	13	190	730	1530	1960	5.7	320	16	557	154 900	0.2	1900
Phloem sap (4)	510	490	5.9	23	470	520	660	0.1	430	20	2340	125 900	7	2340
Root	460	300	14	95	680	610	410	5.5	77	10	123	4780	9.7	120
Twigs (1)	690	420	27	190	550	2320	1830	6.2	64	11	22	4670	6.2	64
Twigs (2)	710	270	51	200	700	1190	3740	4.7	190	30	46	8610	6.8	94
Wood (1)	180	99	16	62	230	490	490	1	5	8.7	2.4	250	1.6	8
Wood (2)	260	250	14	62	280	330	430	3.3	47	8	11	880	2.3	12

Results were obtained with ICP-AES. Na, sodium; Mg, magnesium; Al, aluminium; P, phosphorus; S, sulphur; K, potassium; Ca, calcium; Cr, chromium; Mn, manganese; Fe, iron; Co, cobalt; Ni, nickel; Cu, copper; Zn, zinc. Numbers in brackets denote separate samples analysed.

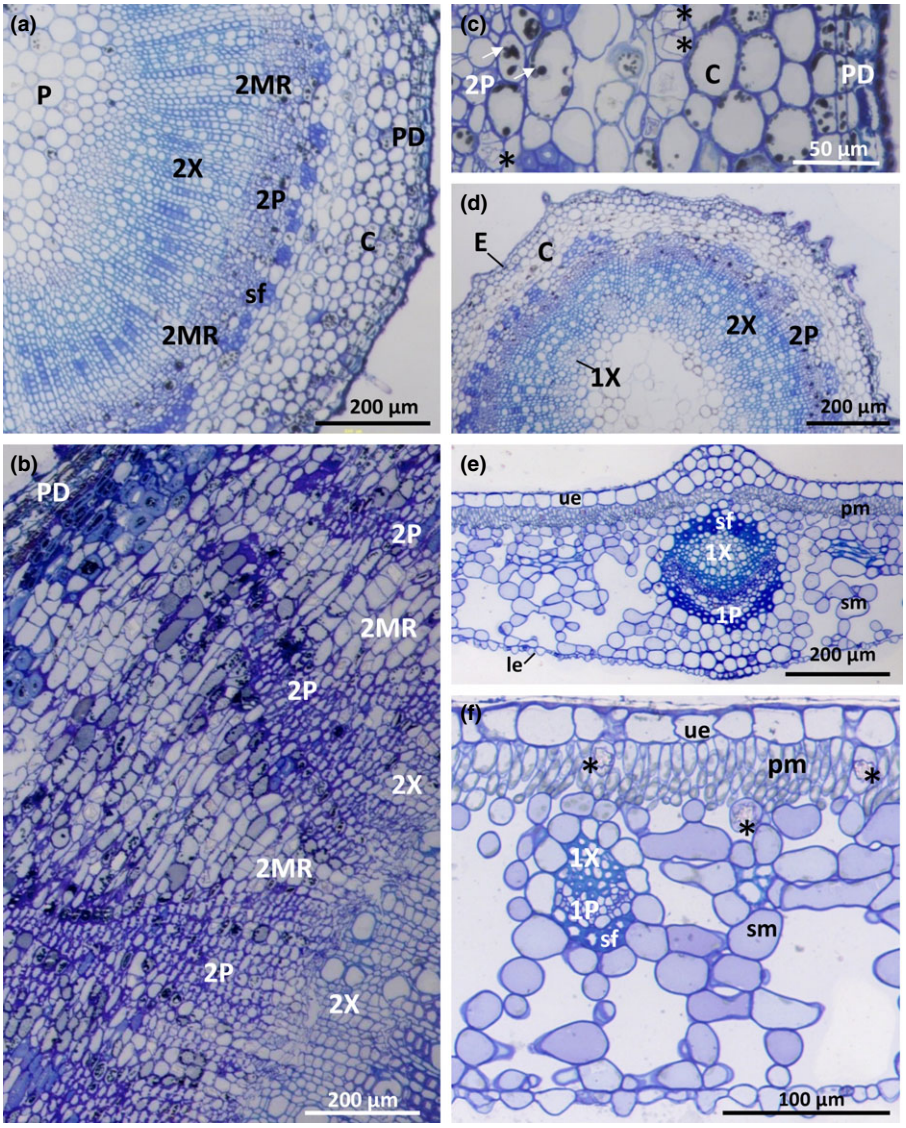

Fig. 2 Light microscopy images of *Phyllanthus balgooyi* anatomical structures. (a) Stem of a young branch, (b) periderm (bark) and underlying tissues of a mature stem, (c) close-up of a young stem showing early periderm formation, (d) anatomical structure of the petiole, (e) mid region of a mature leaf, and (f) close-up of a portion of a mature leaf. C, cortex; E, epidermis; le, lower epidermis; P, pith; PD, periderm; pm, palisade mesophyll; sf, sclerenchyma fibres; sm, spongy mesophyll; ue, upper epidermis; 1P, primary phloem; 1X primary xylem; 2MR, secondary medullary/vascular rays; 2P, secondary phloem; 2X, secondary xylem. Asterisks in (c, f) mark calcium oxalate crystals. Arrows in (c) indicate osmiophilic (black) deposits.

variants that warrant subspecies status, based on their morphologies and the distinct ecological niches they occupy (van der Ent *et al.*, 2015a). In Sabah, populations of *P. balgooyi* from closed forest, montane ridges and riparian habitats all hyperaccumulate Ni, and display an array of growth forms, from shrub to medium-height tree.

Studies on the spatial elemental distribution in tissues and cells have been performed for < 10% of the 450 Ni hyperaccumulator plant species known globally, mainly for small, herbaceous plants. Most investigations were performed on plant species from the families Brassicaceae and Asteraceae (e.g. *Alyssum*, *Thlaspi*, *Berkheya* and *Senecio*) and the leaves were typically the analysed organs, while stems and roots were less often studied (Mesjasz-Przybylowicz *et al.*, 1994, 1996a,b, 1997a,b,c, 2001b; Küpper *et al.*, 2001; Broadhurst *et al.*, 2004, 2009; McNear *et al.*, 2005; Mesjasz-Przybyłowicz *et al.*, 2007; Tappero *et al.*, 2007; Tylko *et al.*, 2007). The only woody shrub analysed to date was *Hybanthus floribundus* (Violaceae) (Bidwell *et al.*, 2003; Kachenko *et al.*, 2008).

In the majority of investigated Ni hyperaccumulator plant species, Ni is preferentially accumulated in the epidermal cells of the shoots, in particular in the foliar epidermal cells (Mesjasz-Przybylowicz *et al.*, 1994, 1996a,b, 1997a,c, 2001b; Küpper *et al.*, 2001; Bidwell *et al.*, 2003; Bhatia *et al.*, 2004; Broadhurst *et al.*, 2004; Tylko *et al.*, 2007; Kachenko *et al.*, 2008).

A distinctly different Ni accumulation pattern has been found in *Berkheya coddii* (Asteraceae) from South Africa (Mesjasz-Przybylowicz *et al.*, 2001a; Mesjasz-Przybyłowicz & Przybyłowicz, 2003, 2011; Budka *et al.*, 2005). In this species, Ni is strongly enriched in the leaf veins and mesophyll, while the concentrations in the epidermis are lower than the average value for the whole leaf (Mesjasz-Przybyłowicz & Przybyłowicz, 2011). A combination of Ni ligand complexation with carboxylic acids at tissue level, and cellular compartmentalization, is involved in detoxification and tolerance mechanisms in most Ni-hyperaccumulating plants (Schaumlöffel *et al.*, 2003; Callahan *et al.*, 2006, 2012; Montargès-Pelletier *et al.*, 2008; McNear *et al.*, 2010). The case of *P. balgooyi* presents one of the most extreme examples of trace element hyperaccumulation. The aim of this study was to elucidate patterns of elemental distribution in the tissues of *P. balgooyi* from Sabah by means of the nuclear microprobe (micro-PIXE) technique.

This is the first study on the elemental distribution in an Ni hyperaccumulator tree species thereby presenting quantitative elemental data for the leaves, petioles and stem. This information may shed light on Ni compartmentalization in this species and the possible chemical forms of Ni in *P. balgooyi* by examining elemental codistribution.

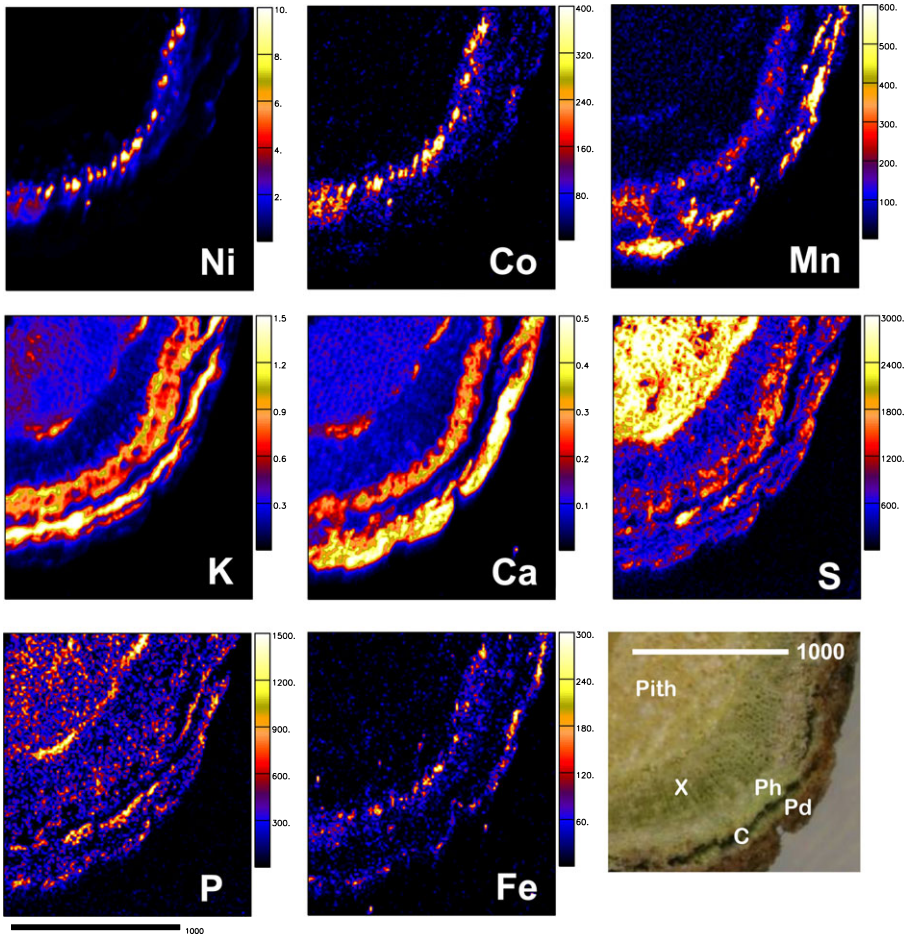

Fig. 3 Quantitative elemental maps and anatomical structure of a stem cross-section of *Phyllanthus balgooyi*. The concentration scale is in wt% DW for nickel (Ni), potassium (K) and calcium (Ca) and μg g^{-1} DW for cobalt (Co), manganese (Mn), sulphur (S), phosphorus (P) and iron (Fe). X, xylem; C, cortex; Ph, phloem; Pd, periderm. Bars, 1000 μm.

Materials and Methods

Collection and analysis of plant tissues

Plant tissue samples of *Phyllanthus balgooyi* Petra Hoffm. & A. J. M. Baker were collected in the natural habitat in the Bukit Hampuan Forest Reserve in Sabah (Malaysia) on the island of Borneo. The following parts were collected from the same individuals: roots, wood, leaves and phloem tissue and phloem sap. The plant tissue samples were cut out with a surgical stainless steel knife directly from the living plants. The samples intended for micro-PIXE analysis were (in the field) immediately flash-frozen using a cold mirror technique in which the samples were pressed between a large block of copper metal cooled by liquid nitrogen (−196°C) and a second block of copper attached to a Teflon holder. This ensured extremely fast freezing of the plant tissue samples to prevent cellular damage by ice crystal formation. The samples were then wrapped in aluminium foil, and transported in a cryogenic container to iThemba LABS, Somerset West, South Africa for analysis. Phloem sap was collected with glass capillary tubes (0.2 mm diameter and 50 mm long) and freeze-dried after collection at −50°C for 8 h.

Plant tissue subsamples were dried at 70°C for 5 d in a dehydrating oven for bulk elemental analysis. These samples were subsequently packed for transport to Australia and gamma-irradiated at Steritech Pty Ltd (Brisbane) following quarantine regulations in Australia. The dried plant tissue samples were subsequently ground and a 300-mg fraction was digested using 5 ml of concentrated nitric acid (70%) and 1 ml of hydrogen peroxide (30%) in a digestion microwave oven (Milestone Start D, Milestone Srl Sorisole, Italy) for a 45-min programme, and after cooling diluted to 30 ml with deionized water. The samples were then analysed by inductively coupled plasma atomic emission spectroscopy (ICP-AES) (Varian Vista Pro II, Agilent Technologies Inc. Palo Alto, USA) for Ni, cobalt (Co), chromium (Cr), copper (Cu), zinc (Zn), manganese (Mn), iron (Fe), manganese (Mg), calcium (Ca), sodium (Na), potassium (K), sulphur (S) and phosphorus (P).

Collection and analysis of bedrock and soil

Soil samples were collected in the rooting zone ('rhizosphere') and under the canopy of *P. balgooyi*, both in the organic horizon and in the mineral soil, in the natural habitat on Bukit Hampuan. Fractions (200 mg) were digested using freshly prepared 'reverse' aqua regia (9 ml of 70% nitric acid and 3 ml of 37% hydrochloric acid per sample) in a digestion microwave for a 2-h programme and diluted with deionized water to 45 ml before analysis to give 'pseudo-total' elemental concentrations. A bedrock sample was also collected at the same location, and a powdered subsample (100 mg) digested with 4 ml of 70% nitric acid, 3 ml of 37% hydrochloric acid and 2 ml of 32% hydrofluoric acid in a microwave for a 2-h programme and diluted to 45 ml before analysis. Soil pH and electrical conductivity (EC) were measured in a 1 : 2.5, soil : water mixture. Phytoavailable metals were extracted with diethylene triamine pentaacetic acid (DTPA) according to

Table 3 Elemental concentrations (micro-PIXE; $\mu g\ g^{-1}$ DW) in the representative specimens of the stem of *Phyllanthus balgooyi* from Sabah (Malaysia)

Tissue	P	S	Cl	K	Ca	Mn	Fe	Co	Ni	Cu	Zn
	$\mu g\ g^{-1}$ (DW)										
Whole area	252 ± 12	1260 ± 40	2450 ± 46	4370 ± 39	1590 ± 20	95 ± 2	11 ± 1	18 ± 2	5670 ± 68	18 ± 3	46 ± 2
Outer periderm (phellem)	255 ± 19	780 ± 30	800 ± 18	3090 ± 28	3390 ± 20	274 ± 2	24 ± 1	10 ± 2	1660 ± 25	14 ± 2	39 ± 2
Inner periderm (phellogen and phelloderm)	1000 ± 110	2600 ± 110	17 960 ± 190	23 000 ± 330	2520 ± 90	116 ± 24	< 17	< 19	2600 ± 90	< 32	< 26
Cortex	214 ± 11	750 ± 30	4730 ± 85	6260 ± 66	1160 ± 17	84 ± 4	12 ± 3	33 ± 5	10 600 ± 140	28 ± 7	88 ± 4
Phloem (1)	< 150	1260 ± 140	4460 ± 144	7960 ± 97	2570 ± 44	160 ± 19	< 24	230 ± 33	78 930 ± 610	< 88	360 ± 40
Phloem (2)	< 180	1160 ± 120	4010 ± 170	6760 ± 67	2670 ± 40	180 ± 18	< 29	290 ± 64	90 500 ± 690	< 110	460 ± 60
Phloem (3)	< 170	970 ± 60	3980 ± 190	6410 ± 85	2790 ± 41	280 ± 20	67 ± 18	360 ± 58	94 060 ± 820	< 110	450 ± 50
Xylem	330 ± 40	750 ± 35	680 ± 16	2350 ± 24	763 ± 9	31 ± 0.9	6.9 ± 1	3 ± 1	1450 ± 20	11 ± 1	12 ± 1
Pith	350 ± 20	2990 ± 74	3710 ± 33	4570 ± 57	1330 ± 23	40 ± 1	1.9 ± 0.8	2 ± 1	840 ± 20	10 ± 1	13 ± 1

Elemental images of this specimen are shown in Fig. 3. The results were obtained from PIXE spectra extracted from regions representing different morphological structures, and analysed using GeoPIXE software. Numbers in brackets denote individual areas analysed. Measured values are shown with errors. P, phosphorus; S, sulphur; Cl, chlorine; K, potassium; Ca, calcium; Mn, manganese; Fe, iron; Co, cobalt; Ni, nickel; Cu, copper; Zn, zinc.

Lindsay & Norvell (1978), but with modifications from Becquer *et al.* (1995) (excluding triethanolamine; pH adjusted to pH 5.3). The digests and extracts were analysed with ICP-AES (Varian Vista Pro II) for Ni, Co, Cu, Zn, Mn, Fe, Mg, Ca, Na, K, S and P.

Micro-PIXE experiments

Specimens were removed from the LN_2 storage container and freeze-dried in a Leica EM CFD Cryosorption Freeze Dryer (Leica Microsystems AG, Vienna, Austria). The freeze-drying process followed a long, 208-h programmed cycle to prevent shrinkage of the tissues. Freeze-dried plant tissues were then hand-cut with a steel razor blade and mounted on specimen holders covered with 0.5% Formvar film (Sigma-Aldrich Chemie GmbH, Schnelldorf, Germany) and lightly coated with carbon to prevent charging. Three individual samples of leaves, petioles and stems were analysed by PIXE. Microanalyses were performed using the nuclear microprobe at the Materials Research Department, iThemba LABS, South Africa. The facility and methodology for measurements of biological materials have been reported elsewhere in detail (Prozesky *et al.*, 1995; Przybyłowicz *et al.*, 1999, 2005). To summarize: a proton beam of 3-MeV energy, provided by a 6-MV single-ended Van de Graaff accelerator, was focused to a $3 \times 3\ \mu m^2$ spot and raster scanned over the areas of interest, using square or rectangular scan patterns with a variable number of pixels (up to 128×128). The proton current was restricted to 100–150 pA to minimize specimen beam damage. Particle-induced X-ray emission (PIXE) and proton backscattering spectrometry (BS) were used simultaneously. PIXE spectra were registered with a Si(Li) detector manufactured by PGT (Princeton, NJ, USA) (30-mm^2 active area and 8.5-μm Be window) with an additional 125-μm Be layer as an external absorber. The effective energy resolution of the PIXE system (for the Mn Kα line) was 160 eV, measured for individual spectra. The detector was positioned at a takeoff angle of 135° and a working distance of 24 mm. The X-ray energy range was set between 1 and 40 keV. BS spectra were recorded with an annular Si surface barrier detector (100 μm thick) positioned at an average angle of 176°. Data were acquired in the event-by-event mode. The normalization of results was performed using the integrated beam charge, collected simultaneously from a Faraday cup located behind the specimen and from the insulated specimen holder. The total accumulated charge per scan varied from 0.51 to 3.82 μC.

The experimental conditions made it possible to quantitatively analyse the concentration and distribution of the following elements in the freeze-dried plant tissues of *P. balgooyi*: silicon (Si), P, S, chlorine (Cl), K, Ca, Cr, Mn, Fe, Co, Ni, Cu, Zn, bromine (Br), rubidium (Rb) and strontium (Sr). These quantitative results were obtained by a standardless method using the GeoPIXE II software package (Ryan *et al.*, 1990a,b; Ryan, 2000). The error estimates were extracted from the error matrix generated in the fit, and the minimum detection limits (MDLs) were calculated using the Currie equation (Currie, 1968). The detailed calibration of detector efficiency, the thicknesses of selectable X-ray attenuating filters and results of studies on the accuracy and precision have been reported elsewhere (van Achterbergh *et al.*, 1995). The procedure reported by van Achterbergh *et al.* (1995) was used for the PGT Si(Li) detector in the present study. The calibration of the analytical system was tested by measurements of standards – pure elements and synthetic glasses with known quantities of selected minor elements (internal standards), the X-ray peaks of which cover practically the whole measurable energy range. Quantitative elemental mapping was performed using

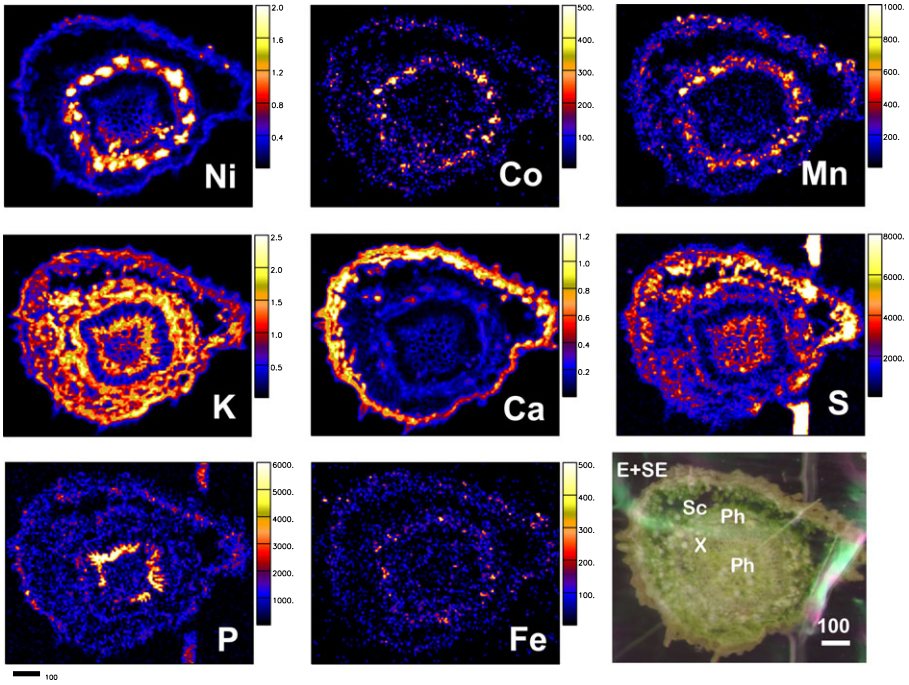

Fig. 4 Quantitative elemental maps and anatomical structure of a petiole cross-section of *Phyllanthus balgooyi*. The concentration scale is in wt% DW for nickel (Ni), potassium (K) and calcium (Ca) and μg g^{-1} DW for cobalt (Co), manganese (Mn), sulphur (S), phosphorus (P) and iron (Fe). E + SE, epidermis and subepidermis; Sc, sclerenchyma; Ph, phloem; X, xylem. Bars, 100 μm.

the dynamic analysis method (Ryan & Jamieson, 1993; Ryan *et al.*, 1995; Ryan, 2000). This method generates elemental images which are overlap-resolved, with subtracted background, and quantitative, that is, accumulated in $\mu g\,g^{-1}$ DW units. Maps were complemented by data extracted from arbitrarily selected microareas within scanned plant tissue. PIXE and BS spectra were employed to obtain average concentrations from these microareas using a full nonlinear deconvolution procedure to fit PIXE spectra (Ryan *et al.*, 1990a,b), with matrix corrections based on thickness and matrix composition obtained from the corresponding BS spectra, fitted with the RUMP simulation package (Doolittle, 1986) with non-Rutherford cross-sections for C, O and N.

Anatomical studies

Plant tissue samples were taken from stems of young branches, the outermost portions of older/main stems, petioles, and mature leaf blades. These were fixed in 3% glutaraldehyde, post-fixed in 2% osmium tetraoxide (OsO_4), dehydrated in a graded ethanol series and embedded in Spurr's (1969) resin. Sections of 0.5–2 μm thickness were cut with a diamond knife, stained with azur II and methylene blue, and examined and photographed with a compound microscope.

Results

Habitat of *P. balgooyi* at the study locality

The plant tissues analysed in this study originated from Bukit Hampuan Forest Reserve in Sabah, Malaysia. At this location, a large population of *P. balgooyi* occurs on a narrow forested ridge on the top of a hill at 1270 m above sea level, with individuals reaching heights of up to 9 m, with stem diameters up to 20 cm (Fig. 1). The forest is semiclosed with a broken canopy dominated by *Dacrydium pectinatum* (Podocarpaceae) and is extremely species-rich (van der Ent *et al.*, 2015b). The vegetation is undisturbed old-growth forest in local climax. As far as is known, no other Ni hyperaccumulator species occur in the same habitat. *Phyllanthus balgooyi* occurs as scattered individuals with numerous small saplings, but flowering has not been observed and is presumed to occur rarely.

The soil at the *P. balgooyi* habitat is shallow (< 40 cm), stony and derived from strongly serpentinized ultramafic (peridotite) bedrock with a major composition of: 4.5 wt% aluminium (Al), 2.4 wt% Ca, 10.3 wt% Fe, 46 wt% Mg (Table 1) and 19.7 wt% Si (data not shown). Concentrations of trace elements in the bedrock are: 20 $\mu g\,g^{-1}$ Co and 1112 $\mu g\,g^{-1}$ Ni, but these elements are strongly enriched during soil formation (compare with soil values in Table 2). The mineral soil is near neutral at pH 6.4 with pseudo-total elemental concentrations of 173–561 $\mu g\,g^{-1}$ Co and 1623–1860 $\mu g\,g^{-1}$ Ni, whereas the organic soil has 339 $\mu g\,g^{-1}$ Co and 887 $\mu g\,g^{-1}$ Ni. The rhizosphere soil is more acidic (pH 5.1) and Co and Ni are depleted (71 and 583 $\mu g\,g^{-1}$, respectively), which may point to a diffusion

Table 4 Elemental concentrations (micro-PIXE; $\mu g\,g^{-1}$ DW) in the representative specimens of the petiole of *Phyllanthus balgooyi* from Sabah (Malaysia)

Tissue	P	S	Cl	K	Ca	Mn	Fe	Co	Ni	Cu	Zn
	$\mu g\,g^{-1}$ (DW)										
Whole area	640 ± 23	2380 ± 70	6620 ± 100	12 000 ± 100	2870 ± 70	160 ± 6	18 ± 3	16 ± 6	6000 ± 100	13 ± 4	86 ± 4
Phloem (1)	970 ± 240	1080 ± 230	6370 ± 330	10 850 ± 320	1100 ± 140	1600 ± 100	< 87	460 ± 150	10 3300 ± 1500	< 300	620 ± 120
Phloem (2)	< 400	1300 ± 150	5650 ± 230	15 080 ± 190	1950 ± 90	740 ± 60	< 65	240 ± 100	67 700 ± 1100	< 230	493 ± 100
Phloem (3)	< 405	1640 ± 160	6240 ± 180	11 030 ± 300	4450 ± 130	870 ± 80	< 60	< 95	36 300 ± 990	< 210	327 ± 90
Phloem (4)	< 455	1280 ± 160	4750 ± 300	16 480 ± 210	3900 ± 110	630 ± 70	< 66	340 ± 100	55 600 ± 1200	< 240	< 175
Phloem (5)	< 420	2280 ± 410	6620 ± 190	12 320 ± 270	2200 ± 90	570 ± 60	< 65	370 ± 70	75 600 ± 1600	< 270	< 215
Phloem (6)	< 430	2340 ± 410	6700 ± 190	12 320 ± 270	2200 ± 90	570 ± 60	< 65	370 ± 70	75 600 ± 1700	< 270	< 215
Epidermis and subepidermis	490 ± 60	3170 ± 110	7530 ± 80	9780 ± 70	9000 ± 70	214 ± 7	24 ± 3	12 ± 6	3350 ± 60	< 9	99 ± 5
Sclerenchyma (1)	< 550	3840 ± 350	13 340 ± 310	16 880 ± 300	1280 ± 100	165 ± 50	< 40	< 50	4560 ± 200	< 130	< 160
Sclerenchyma (2)	< 510	3920 ± 280	11 420 ± 270	17 810 ± 360	1180 ± 80	190 ± 100	< 41	< 54	5110 ± 220	< 150	< 190
Sclerenchyma (3)	< 460	3020 ± 220	13 400 ± 430	11 120 ± 190	1160 ± 70	230 ± 40	< 36	< 46	1570 ± 120	< 150	< 170
Cortex	< 120	2170 ± 90	8970 ± 80	12 180 ± 90	2210 ± 70	107 ± 8	< 7	< 9	1090 ± 60	< 16	35 ± 9
Xylem	710 ± 100	760 ± 30	2100 ± 40	5250 ± 40	530 ± 20	52 ± 6	< 5	< 5	2640 ± 40	< 11	17 ± 4
Primary xylem and parenchyma	7200 ± 600	2810 ± 150	2040 ± 100	17 120 ± 200	1540 ± 120	59 ± 15	< 13	< 16	2700 ± 140	< 30	< 28
Pith	470 ± 50	2870 ± 100	4520 ± 70	9350 ± 130	1240 ± 40	66 ± 5	< 6	< 7	2900 ± 60	< 13	< 10

Elemental images of this specimen are shown in Fig. 4. The results were obtained from PIXE spectra extracted from regions representing different morphological structures, and analysed using GeoPIXE software. Numbers in brackets denote individual areas analysed. Measured values are shown with errors. P, phosphorus; S, sulphur; Cl, chlorine; K, potassium; Ca, calcium; Mn, manganese; Fe, iron; Co, cobalt; Ni, nickel; Cu, copper; Zn, zinc.

gradient towards the roots, especially because Al and Fe concentrations are high (148 and 278 $\mu g\,g^{-1}$, respectively), suggestive of exudate-induced mineral weathering. Phytoavailability (DTPA-extractable) of Ni is moderately high at 177–291 $\mu g\,g^{-1}$ in the mineral soil and 98 $\mu g\,g^{-1}$ in the organic soil.

Bulk elemental concentrations in plant tissues of *P. balgooyi*

The results of the bulk elemental concentrations are shown in Table 2. Compared with many other Ni hyperaccumulator plant species, the leaves of *P. balgooyi* did not contain exceptionally high Ni concentrations (4900–7060 $\mu g\,g^{-1}$ Ni) and Co was low at 20–46 $\mu g\,g^{-1}$. However, Ca was very high in the leaves at 6800–8680 $\mu g\,g^{-1}$. Ni concentrations in green twigs were high at 4700–8600 $\mu g\,g^{-1}$, which may be explained by the presence of phloem tissue. The bark contained little Ni (360–370 $\mu g\,g^{-1}$) and was also low in Ca (95–116 $\mu g\,g^{-1}$), whereas wood had 250–880 $\mu g\,g^{-1}$ Ni. The root Ni concentration was 4800 $\mu g\,g^{-1}$ and phloem tissue contained 45 000 $\mu g\,g^{-1}$ Ni and 250 $\mu g\,g^{-1}$ Co. The phloem sap from *P. balgooyi* is one of the most remarkable biological liquids in the world. It is exudated as a clear dark-green viscous sap when the phloem tissue is damaged (under a very thin scaling bark). The phloem sap contained 12.6–16.9 wt% Ni and was also strongly enriched in Co (560–2340 $\mu g\,g^{-1}$). Although concentrations of most other transition elements were low (Fe: 15–20 $\mu g\,g^{-1}$; Cr: 0.1–5.7 $\mu g\,g^{-1}$; Cu: 0.2–7 $\mu g\,g^{-1}$; Mn: 320–480 $\mu g\,g^{-1}$), concentrations of Zn were very high (1900–3700 $\mu g\,g^{-1}$). The level of specificity for Ni over other transition elements, except Co and Zn, suggests the activity of highly selective transporters.

Anatomical features of *P. balgooyi* stems and leaves

Typical of woody plants, transporting tissues, in particular secondary xylem and phloem, make up a large proportion of the stem of *P. balgooyi* (Fig. 2a,c). As a consequence of secondary growth, the epidermis is replaced by a periderm (bark), which forms the outermost tissue (Fig. 2a–c). Petioles have a similar anatomical structure as that of young stems but do not usually form a periderm (Fig. 2d). Leaves (Fig. 2e,f) are dorsiventral with a narrow palisade mesophyll layer (two to four cells wide) located on the upper side adjacent to the upper epidermis. Spongy mesophyll occupies a large proportion of the leaf blade, extending from the palisade tissues to the lower epidermis. The latter is unusual in that it is composed of very small cells, three to six times smaller than those of the upper epidermis.

Calcium oxalate crystals (mainly in the form of druses and prismatic crystals) occur in the stem and leaf tissues. In the stems they are found in cells of the cortex and phloem (Fig. 2b,f, asterisks), while in leaves they are located within palisade and spongy mesophylll cells (Fig. 2f, asterisks) as well as in the phloem cells of major veins. Osmiophilic (black) deposits (Fig. 2b, arrows) occur in cells of tissues where calcium oxalate crystals form.

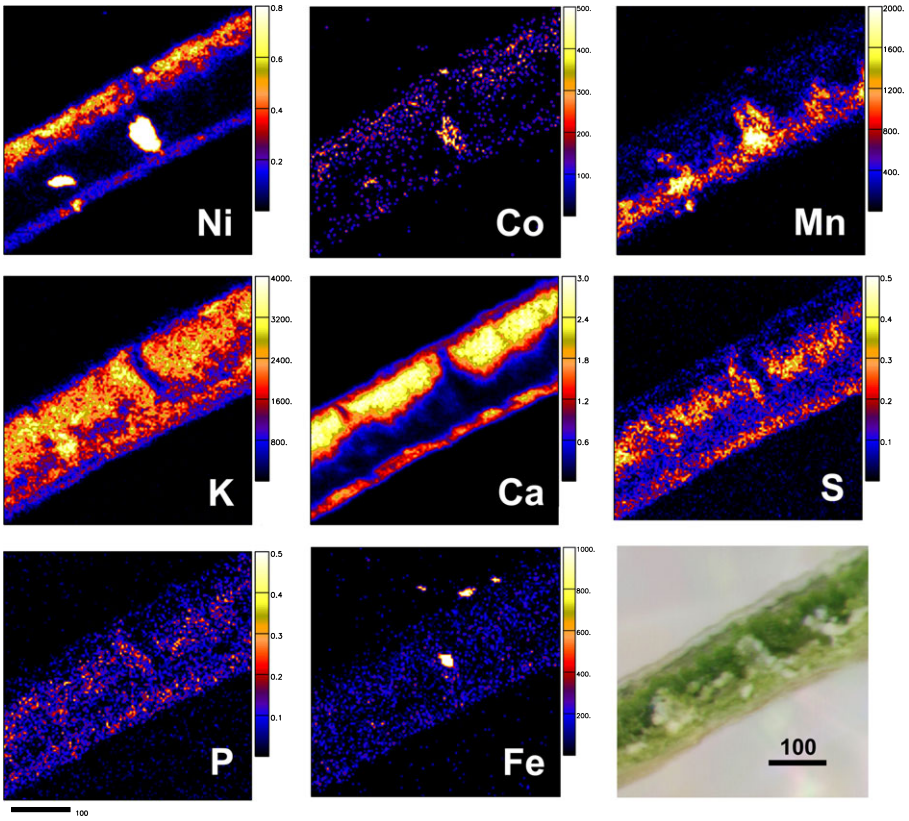

Fig. 5 Quantitative elemental maps and anatomical structure of a leaf cross-section of *Phyllanthus balgooyi*. The concentration scale is in wt% DW for nickel (Ni), calcium (Ca), sulphur (S) and phosphorus (P) and $\mu g\,g^{-1}$ DW for cobalt (Co), manganese (Mn), potassium (K) and iron (Fe). Bars, 100 μm.

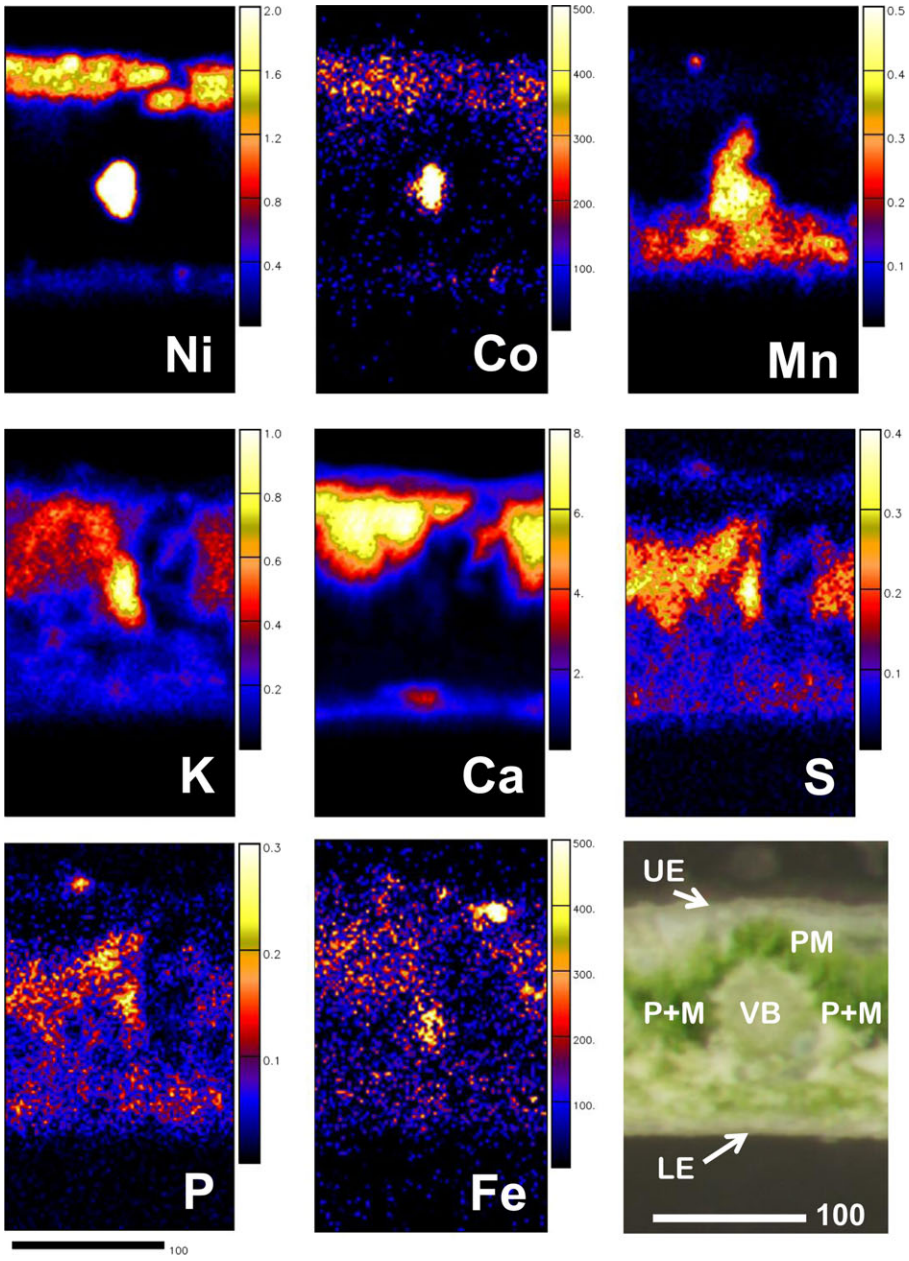

Fig. 6 Quantitative elemental maps and anatomical structure of an enlarged part of a leaf cross-section of *Phyllanthus balgooyi*. The concentration scale is in wt% DW for nickel (Ni), manganese (Mn), potassium (K), calcium (Ca), sulphur (S) and phosphorus (P) and $\mu g\, g^{-1}$ DW for cobalt (Co) and iron (Fe). EU, upper epidermis; LE, lower epidermis; VB, vascular bundle; P + M, parenchyma and mesophyll; PM, palisade mesophyll. Bars, 100 μm.

Elemental distribution in plant tissues of *P. balgooyi*

Phyllanthus balgooyi has very well-developed phloem tissue which has a dark-green colour from the presence of Ni ions. Analysis of stem sections of *P. balgooyi* (Fig. 3; Table 3) showed that the Ni concentration was very high in the phloem, reaching up to 9.4 wt%. The Fe, Co, Cu and Zn distributions mirrored that of Ni, with significant enrichment in the phloem (Cu and Zn maps not shown), but their concentrations were much lower, up to 67 $\mu g\, g^{-1}$ for Fe, 360 $\mu g\, g^{-1}$ for Co and 460 $\mu g\, g^{-1}$ for Zn. Fe was also somewhat enriched in the outer part of the periderm (phellem, 24 $\mu g\, g^{-1}$). Ca had two enrichment areas, the outer periderm (phellem) and phloem. The concentrations in the outer periderm were higher than in the phloem, at 0.34 and 0.28 wt%, respectively. Mn also showed enrichment in the outer periderm and phloem, but at much lower concentrations of 274 $\mu g\, g^{-1}$ and up to 280 $\mu g\, g^{-1}$, respectively. K reached the highest values in the relatively thin inner periderm (phellogen and phelloderm), up to 2.3 wt% (Table 3). Phloem was another tissue where K showed enrichment, although with somewhat lower concentrations, of the order of 0.6–0.8 wt%. S and P had the highest values in the pith, at 0.3 wt% and 350 $\mu g\, g^{-1}$, respectively.

Analysis of the petiole (Fig. 4; Table 4) showed that Ni attained the highest concentrations again in the phloem, reaching up to 10.3 wt%. Some enrichment could be also observed in the epidermis and subepidermis, but the concentrations there did not exceed 0.34 wt%. Mn, Co, Zn (Zn map not shown) and to some extent Fe followed the same distribution pattern as

Ni and in the phloem attained concentrations of up to 1600 μg g^{-1} for Mn, 460 μg g^{-1} for Co, and 620 μg g^{-1} for Zn. The enrichment of these elements in the epidermis and subepidermis was much lower: 214 μg g^{-1} for Mn, 24 mg kg^{-1} for Fe, 12 μg g^{-1} for Co and 99 mg kg^{-1} for Zn. Ca showed a very clear enrichment pattern in the epidermis and subepidermis (0.9 wt%). It also showed some enrichment in the phloem, but this did not exceed 0.45 wt%. K, S and Cl were distributed more homogeneously than any of the other elements, but were clearly depleted in the xylem. P showed an enrichment pattern in the primary xylem and parenchyma, with a concentration exceeding 0.7 wt%.

In the leaves, Ni showed a very significant enrichment in the vascular bundles (Figs 5, 6; Table 5), up to 8.9 wt%. Another area of Ni enrichment in the leaves was the upper epidermis, but the concentration there did not exceed 1.3 wt%. Ni concentrations in the lower epidermis and palisade mesophyll were 0.25 wt% and 500 μg g^{-1}, respectively. The lowest Ni concentrations were found in the spongy mesophyll, not exceeding 130 μg g^{-1}. Co was the only element that mirrored the distribution of Ni. It showed enrichment in the vascular bundles but only up to 390 μg g^{-1}, while its concentration in the upper and lower epidermis was 81 and 14 μg g^{-1}, respectively. In the palisade and spongy mesophyll, Co concentrations were below the detection limits. The distribution of Mn was in striking contrast with that of Ni and Co. Although the highest concentrations of this element were in the vascular bundle, exceeding 0.4 wt%, it was also significantly enriched in the spongy mesophyll near to the lower epidermis. K showed a much more homogeneous distribution in the spongy mesophyll than any other element. It attained the highest concentrations in the vascular bundles (> 0.7 wt%). Both epidermal regions were K-depleted. P and to a lesser extent S mirrored the distribution of K. Ca showed enrichment in the upper epidermis (5.4 wt%) and palisade mesophyll (3.9 wt%). The lower epidermis was another tissue type with substantial Ca enrichment, where concentrations reached 1.8 wt%.

Discussion

The results of this study show that in *P. balgooyi* Ni has a highly distinctive spatial distribution with extreme levels of accumulation in the vascular tracts (leaves) and phloem bundles (stem and petiole). The phloem tissue of the main stem of *P. balgooyi* is literally green from Ni ions and appears to act as a 'sink', with Ni concentrations reaching up to 9.4 wt% (Fig. 3; Table 3), whereas sap exuding from this tissue reached up to 16.9 wt% Ni (Fig. 1; Table 2). This type of Ni distribution is very different from those of all other known Ni hyperaccumulator plants, except for the tree *Pycnandra acuminata* from New Caledonia, which also has an Ni-rich phloem and latex exudate. In *P. balgooyi*, concentrations attained much higher values (up to 10.3 wt%) in the phloem of the petiole, contrasting strikingly with the adjoining sclerenchyma, where Ni values were an order of magnitude lower (Fig. 4; Table 4). The findings of previous investigations reporting on the elemental distribution in the stems and petioles of Ni hyperaccumulator plants

Table 5 Elemental concentrations (micro-PIXE; μg g^{-1} DW) in the representative specimens of leaf cross-sections of *Phyllanthus balgooyi* from Sabah (Malaysia)

Tissue	P	S	Cl	K	Ca	Mn	Fe	Co	Ni	Cu	Zn
	μg g^{-1} (DW)										
Whole area	540 ± 20	1080 ± 45	8750 ± 100	2680 ± 40	23 140 ± 170	1045 ± 20	52 ± 3	45 ± 5	6000 ± 100	10 ± 4	24 ± 2
Vascular bundle	1160 ± 150	2080 ± 120	20 340 ± 460	7180 ± 110	5610 ± 70	4310 ± 80	< 26	390 ± 56	89 320 ± 1300	< 83.	< 54
Upper epidermis	160 ± 40	500 ± 30	3720 ± 40	2780 ± 35	53 560 ± 350	255 ± 7	72 ± 10	81 ± 6	12 640 ± 200	< 16	< 11
Lower epidermis	650 ± 50	1100 ± 70	11 560 ± 170	1740 ± 40	17 580 ± 210	690 ± 25	16 ± 8	14 ± 6	2470 ± 90	< 14	36 ± 6
Spongy mesophyll (1)	790 ± 40	1540 ± 70	12 170 ± 140	2450 ± 50	6150 ± 70	1000 ± 25	58 ± 6	< 3	126 ± 8	< 7	23 ± 4
Spongy mesophyll (2)	400 ± 20	900 ± 50	7450 ± 90	1970 ± 50	5050 ± 60	1100 ± 26	37 ± 8	< 4	112 ± 5	< 7	< 6
Palisade mesophyll	870 ± 40	1800 ± 40	6640 ± 60	3870 ± 30	39 350 ± 280	390 ± 12	81 ± 6	< 6	500 ± 30	< 13	< 12

The results were obtained from PIXE spectra extracted from regions representing different morphological structures, and analysed using GeoPIXE software. Numbers in brackets denote individual areas analysed. Measured values are shown with errors. P, phosphorus; S, sulphur; Cl, chlorine; K, potassium; Ca, calcium; Mn, manganese; Fe, iron; Co, cobalt; Ni, nickel; Cu, copper; Zn, zinc.

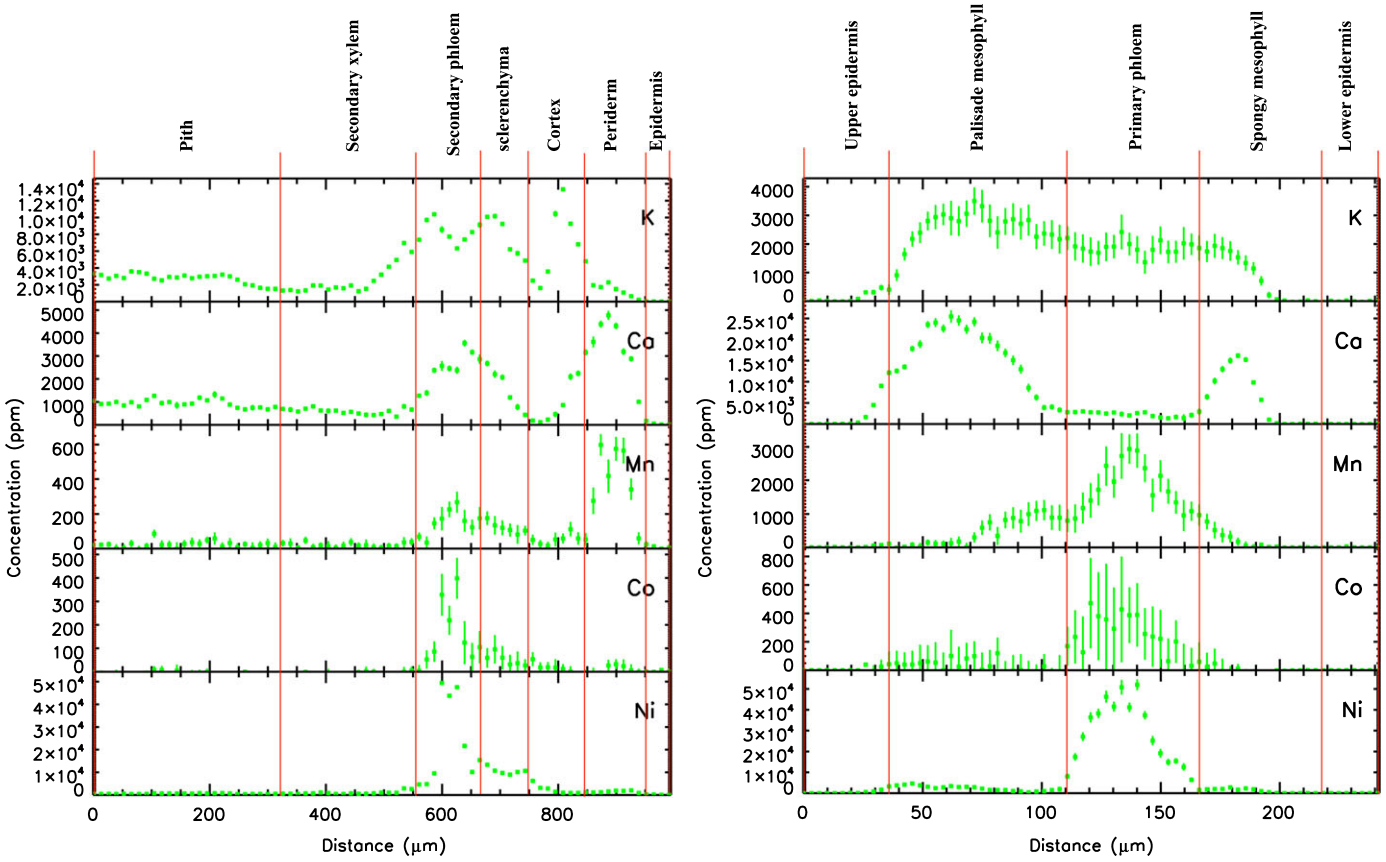

Fig. 7 Transverse section through a stem with concentrations of potassium (K), calcium (Ca), manganese (Mn), cobalt (Co) and nickel (Ni) (left), and transverse through a leaf section with concentrations of K, Ca, Mn, Co and Ni (right). The approximate anatomical features are noted in the sequence over the transverse.

(Mesjasz-Przybylowicz *et al.*, 1994, 1997b,c; Küpper *et al.*, 2001; Bhatia *et al.*, 2004; McNear *et al.*, 2005; Kachenko *et al.*, 2008) are not consistent. Significant Ni enrichment in the phloem has so far only been reported from the stem of *Senecio coronatus* (Mesjasz-Przybylowicz *et al.*, 1997b).

Ni enrichment in the epidermal parts of leaves (Figs 5, 6; Table 5) and the epidermis and subepidermis of petioles (Fig. 4; Table 4) is a typical distribution pattern encountered in the majority of studied Ni hyperaccumulator plants to date. For example, in *Alyssum bertolonii*, *Alyssum lesbiacum*, *Thlaspi goesingense* (Küpper *et al.*, 2001), *Alyssum murale* (Broadhurst *et al.*, 2004, 2009; Tappero *et al.*, 2007; McNear *et al.*, 2010), *Stackhousia tryoni* (Bhatia *et al.*, 2004), *Stackhousia coronatus*, *Stackhousia anomalochrous* and *Berkheya zeyheri* subsp. *rehmannii* var. *rogersiana,* Ni was located mainly in the epidermal parts of the leaves (Mesjasz-Przybylowicz *et al.*, 1994, 1996a,b, 1997a,c, 2001b; Przybylowicz *et al.*, 1995; Tylko *et al.*, 2007).

In the leaves of *Hybanthus floribundus*, the only woody Ni hyperaccumulator investigated with micro-PIXE to date, Ni was preferentially localized in the upper epidermis (Kachenko *et al.*, 2008). Studies at the cellular level revealed that Ni accumulated in the vacuoles of the epidermal cells (Bidwell *et al.*, 2003). The different Ni spatial distribution reported for *Berkheya coddii*, where significant enrichment of Ni was found in vascular bundles and mesophyll, with the lowest concentration in the epidermis, was noted in the Introduction (Mesjasz-Przybyłowicz & Przybyłowicz, 2003, 2011).

Based on these studies, Ni accumulation in the foliar epidermal cells of Ni accumulator plants appears to be a general worldwide characteristic, with the exception of *B. coddii*. The hypothesis of preferential accumulation of Ni in the epidermis to aid herbivory protection (Boyd & Martens, 1992) would only make sense if symmetrical accumulation takes place in both the upper and lower epidermis, as insect herbivores feed on both sides. Robinson *et al.* (2003) suggested that preferential accumulation of Ni in the upper epidermis might act as protection for the underlying chlorophyll against ultraviolet radiation. In *P. balgooyi*, the preferential accumulation of Ni in the upper epidermis extending into the spongy mesophyll means that herbivory protection is unlikely, but that it may act as a UV filter.

The very high concentrations in the vascular bundles of *P. balgooyi* leaves are another anomaly among hyperaccumulators. Although similar patterns were reported for *S. tryonii* (Bhatia *et al.*, 2004), *A. murale* (McNear *et al.*, 2005) and *B. coddii* (Mesjasz-Przybyłowicz & Przybyłowicz, 2011), the contrast between concentrations found in the vascular bundles and the adjoining mesophyll has never been reported as extreme as in *P. balgooyi* (Fig. 7).

Although the resolution of micro-PIXE (3 × 3 μm) is not sufficient to resolve true subcellular elemental patterns, the shape of

the Ni distribution combined with the rather sparsely spaced cells in the upper epidermis (Fig. 6) suggests that Ni is present mainly in the vacuoles. This is consistent with the findings of earlier studies, which also hypothesized vacuolar sequestration as the key mechanism in hyperaccumulator plants (Krämer *et al.*, 2000; Küpper *et al.*, 2001; Bidwell *et al.*, 2003). The fact that Ni is water-soluble, as evidenced by the rapid dissolution of the freeze-dried phloem sap of *P. balgooyi* in water, also supports a vacuolar storage mechanism. In many other Ni hyperaccumulator plants, Ni complexes were water-soluble (Robinson *et al.*, 2003; Montargès-Pelletier *et al.*, 2008). Küpper *et al.* (2001) found a positive correlation between S and Ni in the cells of the hyperaccumulators *A. bertolonii*, *A. lesbiacum* and *T. goesingense* and suggested that complexation with sulphate might be important. A positive correlation between Ni and S was also found in *A. murale* (Broadhurst *et al.*, 2004). However, in *P. balgooyi* the prevailing concentrations of S and P are orders of magnitude lower than Ni and hence neither sulphate nor phosphate is likely to play a significant role in Ni complexation. Moreover, regions of P and S enrichment do not correlate with those of Ni enrichment in the plant tissues of *P. balgooyi*.

In *P. balgooyi*, the distribution of Co mirrored that of Ni, but the distribution of Mn in the leaves differed from that of Ni. By contrast, Broadhurst *et al.* (2009) showed that in *A. murale* and *A. corsicum* Ni and Mn distributions were strongly spatially correlated and the authors suggested that Ni hyperaccumulation in *Alyssum* species might have evolved from an Mn-handling system. In *P. balgooyi*, there was no gradient of Ni concentrations evident across the leaf axis, as was observed in *B. coddii* (Mesjasz-Przybylowicz *et al.*, 2001b) and *Hybanthus floribundus* subsp. *floribundus* (Kachenko *et al.*, 2008) where Ni concentrations were the highest in the leaf margins and the vascular bundles. Kachenko *et al.* (2008) suggested that such patterns (Ni preferential accumulation away from the chlorophyll-rich mesophyll cells in the midrib area) could be a mechanism to minimize interference with photosynthesis. In *P. balgooyi*, the structures where Ni is mainly accumulated are directly above the photosynthetically active palisade mesophyll layer of the leaf. Hence, Ni is still spatially separated from metabolically important processes.

The extreme concentration of Ni in the phloem vessels from leaves to stems probably has a significant effect on the osmotic pressure of the sieve elements. According to the 'pressure flow hypothesis', phloem loading and unloading of sugars (such as sucrose) creates a diffusion gradient through osmosis. The osmotic potential of 16 wt% Ni-citrate solution in the phloem sap could fulfill the role of osmoticum. Ni hyperaccumulation has previously been hypothesized to act as an osmoticum in plant cells to increase drought tolerance by lowering the water potential (Severne, 1974). Bidwell *et al.* (2003) found that the accumulation of Ni in the epidermal vacuoles of *Hybanthus floribundus* subsp. *floribundus* was associated with a decrease in the concentrations of K and Na and with an overall decline in cell water potential. *Phyllanthus balgooyi* grows in a tropical wet climate with abundant year-round rainfall, so this seems unlikely in this case, but the link with nutrient acquisition is intriguing and warrants detailed experimental follow-up studies.

Acknowledgements

We wish to thank David Mulligan, Peter Erskine (UQ), Mark Tibbett (University of Reading, UK) and Alan Baker (University of Melbourne, Australia) for their advice and encouragement. We also wish to thank Rimi Repin, Rositti Karim, Sukaibin Sumail (Sabah Parks, Malaysia) and Postar Miun (Sabah Forestry Department, Malaysia) for their help and expertise in the field. The assistance of Ms Ewa Przybylowicz with the preparation of the figures is gratefully acknowledged. This research was undertaken at the nuclear microprobe facility of iThemba Laboratory for Accelerator Based Sciences in South Africa.

Author contributions

J.M-P. and A.v.d.E. planned and designed the research. A.v.d.E. conducted fieldwork. J.M-P. prepared the samples for micro-PIXE analyses. J.M-P. and W.P. performed micro-PIXE analyses and the data processing and evaluation. A.B. performed anatomical studies. J.M-P., W.P., A.B. and A.v.d.E. wrote the manuscript.

References

van Achterbergh E, Ryan CG, Gurney JJ, Le Roex AP. 1995. PIXE profiling, imaging and analysis using the NAC proton microprobe: unraveling mantle eclogites. *Nuclear Instruments and Methods in Physics Research Section B* **104**: 415–426.

Baker AJM, Brooks RR. 1988. Botanical exploration for minerals in the humid tropics. *Journal of Biogeography* **15**: 221–229.

Baker AJM, Proctor J, van Balgooy MMJ, Reeves RD. 1992. Hyperaccumulation of nickel by the flora of the ultramafics of Palawan, Republic of the Philippines. In: Baker AJM, Proctor J, Reeves RD, eds. *The vegetation of ultramafic (serpentine) soils*. Andover, UK: Intercept, 291–304.

Becquer T, Bourdon E, Pétard J. 1995. Disponibilité du nickel le long d'une toposéquence de sols développés sur roches ultramafiques de Nouvelle-Calédonie. *Comptes Rendus de l'Académie des Sciences: Série 2. Sciences de la Terre et des Planètes* **321**: 585–592.

Bhatia NP, Walsh KB, Orlic I, Siegele R, Ashwath N, Baker AJM. 2004. Studies on spatial distribution of nickel in leaves and stems of the metal hyperaccumulator *Stackhousia tryonii* Bailey using nuclear microprobe (micro-PIXE) and EDXS techniques. *Functional Plant Biology* **31**: 1061–1074.

Bidwell SD, Crawford SA, Woodrow IE, Sommer-Knudsen J, Marshall AT. 2003. Sub-cellular localization of Ni in the hyperaccumulator, *Hybanthus floribundus* (Lindley) F. Muell. *Plant, Cell & Environment* **27**: 705–716.

Boyd RS, Martens SN. 1992. The raison d'etre for metal hyperaccumulation by plants. In: Baker AJM, Proctor J, Reeves RD, eds. *The vegetation of ultramafic (serpentine) soils*. Andover, UK: Intercept, 279–289.

Broadhurst CL, Chaney RL, Angle JS, Erbe EF, Maugel TK. 2004. Nickel localization and response to increasing Ni soil levels in leaves of the Ni hyperaccumulator *Alyssum murale*. *Plant and Soil* **265**: 225–242.

Broadhurst CL, Tappero RV, Maugel TK, Erbe EF, Sparks DL, Chaney RL. 2009. Interaction of nickel and manganese in accumulation and localization in leaves of the Ni hyperaccumulators *Alyssum murale* and *Alyssum corsicum*. *Plant and Soil* **314**: 35–48.

Brooks RR, Anderson C, Stewart R, Robinson B. 1999. Phytomining: growing a crop of a metal. *Biologist* **46**: 201–205.

Brooks RR, Chambers M, Nicks L, Robinson BH. 1998. Phytomining. *Trends in Plant Science* **3**: 359–362.

Budka D, Mesjasz-Przybyłowicz J, Tylko G, Przybyłowicz WJ. 2005. Freeze-substitution methods for Ni localization and quantitative analysis in *Berkheya coddii* leaves by means of PIXE. *Nuclear Instruments and Methods in Physics Research Section B – Beam Interactions With Materials and Atoms* **231**: 338–344.

Callahan DL, Baker AJM, Kolev SD, Wedd AG. 2006. Metal ion ligands in hyperaccumulating plants. *Journal of Biological Inorganic Chemistry* **11**: 2–12.

Callahan DL, Roessner U, Dumontet V, De Livera AM, Doronila A, Baker AJM, Kolev SD. 2012. Elemental and metabolite profiling of nickel hyperaccumulators from New Caledonia. *Phytochemistry* **81**(C): 80–89.

Chaney RL. 1983. Plant uptake of inorganic waste constituents. In: Parr JF, Marsh PB, Kla JM, eds. *Land treatment of hazardous wastes*. Park Ridge, NJ, USA: Noyes Data Corporation, 50–76.

Chaney RL, Angle JS, Broadhurst CL, Peters CA, Tappero RV, Sparks DL. 2007. Improved understanding of hyperaccumulation yields commercial phytoextraction and phytomining technologies. *Journal of Environmental Quality* **36**: 1429–1443.

Currie LA. 1968. Limits for qualitative detection and quantitative determination: application to radiochemistry. *Analytical Chemistry* **40**: 586–593.

Doolittle LR. 1986. A semiautomatic algorithm for proton backscattering analysis. *Nuclear Instruments and Methods in Physics Research Section B – Beam Interactions With Materials and Atoms* **15**: 227–231.

van der Ent A, Baker AJM, Reeves RD, Pollard AJ, Schat H. 2013b. Hyperaccumulators of metal and metalloid trace elements: facts and fiction. *Plant and Soil* **362**: 319–334.

van der Ent A, Baker AJM, van Balgooy MMJ, Tjoa A. 2013a. Ultramafic nickel laterites in Indonesia (Sulawesi, Halmahera): mining, nickel hyperaccumulators and opportunities for phytomining. *Journal of Geochemical Exploration* **128**: 72–79.

van der Ent A, Erskine PD, Sumail S. 2015a. Ecology of nickel hyperaccumulator plants from ultramafic soils in Sabah (Malaysia). *Chemoecology* **25**: 243–259.

van der Ent A, Mulligan D. 2015. Multi-element concentrations in plant parts and fluids of Malaysian nickel hyperaccumulator plants and some economic and ecological considerations. *Journal of Chemical Ecology* **41**: 396–408.

van der Ent A, Repin R, Sugau J, Wong KM. 2015b. Plant diversity of ultramafic outcrops in Sabah (Malaysia). *Australian Journal of Botany* **63**: 204–215.

Harris AT, Naidoo K, Nokes J, Walker T, Orton F. 2009. Indicative assessment of the feasibility of Ni and Au phytomining in Australia. *Journal of Cleaner Production* **17**: 194–200.

Hoffmann P, Baker AJM, Proctor J, Madulid DA. 2003. *Phyllanthus balgooyi* (Euphorbiaceae s.l.), a new nickel-hyperaccumulating species from Palawan and Sabah. *Blumea* **48**: 193–199.

Jaffré T, Brooks RR, Lee J, Reeves RD. 1976. *Sebertia acuminata*: a hyperaccumulator of Nickel from New Caledonia. *Science* **193**: 579–580.

Kachenko AG, Singh B, Bhatia NP, Siegele R. 2008. Quantitative elemental localisation in leaves and stems of nickel hyperaccumulating shrub *Hybanthus floribundus* subsp. *floribundus* using micro-PIXE spectroscopy. *Nuclear Instruments and Methods in Physics Research Section B: Beam Interactions With Materials and Atoms* **266**: 667–676.

Krämer UU, Pickering IJI, Prince RCR, Raskin II, Salt DED. 2000. Subcellular localization and speciation of nickel in hyperaccumulator and non-accumulator *Thlaspi* species. *Plant Physiology* **122**: 1343–1353.

Küpper H, Lombi E, Zhao FJ, Wieshammer G, McGrath SP. 2001. Cellular compartmentation of nickel in the hyperaccumulators *Alyssum lesbiacum*, *Alyssum bertolonii* and *Thlaspi goesingense*. *Journal of Experimental Botany* **52**: 2291–2300.

Lindsay WL, Norvell WA. 1978. Development of DTPA soil test for zinc, iron, manganese, and copper. *Soil Science Society of America Journal* **42**: 421–428.

McNear DH, Chaney RL, Sparks DL. 2010. The hyperaccumulator *Alyssum murale* uses complexation with nitrogen and oxygen donor ligands for Ni transport and storage. *Phytochemistry* **71**: 188–200.

McNear DH, Peltier E, Everhart J, Chaney RL, Sutton S, Newville M, Rivers M, Sparks DL. 2005. Application of quantitative fluorescence and absorption-edge computed microtomography to image metal compartmentalization in *Alyssum murale*. *Environmental Science & Technology* **39**: 2210–2218.

Mesjasz-Przybylowicz J, Balkwill K, Przybylowicz WJ, Annegarn HJ. 1994. Proton microprobe and X-ray fluorescence investigations of nickel distribution in serpentine flora from South Africa. *Nuclear Instruments and Methods in Physics Research B* **89**: 208–212.

Mesjasz-Przybylowicz J, Balkwill K, Przybylowicz WJ, Annegarn HJ, Rama DBK. 1996a. Similarity of nickel distribution in leaf tissue of two distantly related hyperaccumulating species. In: van der Maesen LJG, van de Burgt XM, van Medenbach de Roy JM, eds. *The biodiversity of African plants, Proc. XIVth AETFAT Congress*. Dordrecht, the Netherlands: Kluwer Academic Publishers, 331–335.

Mesjasz-Przybyłowicz J, Barnabas A, Przybyłowicz WJ. 2007. Comparison of cytology and distribution of nickel in roots of Ni-hyperaccumulating and non-accumulating genotypes of *Senecio coronatus*. *Plant and Soil* **293**: 61–78.

Mesjasz-Przybyłowicz J, Przybyłowicz WJ. 2003. Nickel distribution in *Berkheya coddii* leaves by Micro-PIXE and SEM-EDS. *Proceedings of the Microscopy Society of South Africa* **33**: 68.

Mesjasz-Przybyłowicz J, Przybyłowicz WJ. 2011. PIXE and metal hyperaccumulation: from soil to plants and insects. *X Ray Spectrometry* **40**: 181–185.

Mesjasz-Przybylowicz J, Przybylowicz WJ, Pineda CA. 2001a. Nuclear microprobe studies of elemental distribution in apical leaves of the Ni hyperaccumulator *Berkheya coddii*. *South African Journal of Science* **97**: 591–593.

Mesjasz-Przybylowicz J, Przybylowicz WJ, Prozesky VM. 1997a. Nuclear microprobe investigation of Ni distribution in organs and cells of hyperaccumulating plants. In: Jaffré T, Reeves RD, Becquer T, eds. *The ecology of ultramafic and metalliferous areas. Proceedings of the second international conference on serpentine ecology*. Noume´a, New Caledonia: Centre ORSTOM de Noume´a, 223–224.

Mesjasz-Przybylowicz J, Przybylowicz WJ, Prozesky VM, Pineda CA. 1996b. *Elemental distribution in a leaf of* Senecio coronatus. *35th MSSA (Microscopy Society of South Africa) Conference, Durban, 4–6 December 1996. Proceedings 26 (68). ISSN 0250-0418; ISBN 0-620-20704-3*. Department of Anatomy, Faculty of Veterinary Science, Onderstepoort, South Africa: Microscopy Society of Southern Africa.

Mesjasz-Przybylowicz J, Przybylowicz WJ, Prozesky VM, Pineda CA. 1997b. Quantitative micro-PIXE comparison of elemental distribution in Ni-hyperaccumulating and non-accumulating genotypes of *Senecio coronatus*. *Nuclear Instruments and Methods in Physics Research B* **130**: 368–373.

Mesjasz-Przybylowicz J, Przybylowicz WJ, Rama DBK, Pineda CA. 1997c. *Elemental distribution in the Ni hyperaccumulator* – Senecio anomalochrous. *Proceedings of the Microscopy Society of Southern Africa 27(89). ISSN 0250-0418; ISBN 0-620-21836-3*. Department of Anatomy, Faculty of Veterinary Science, Onderstepoort, South Africa: Microscopy Society of Southern Africa.

Mesjasz-Przybylowicz J, Przybylowicz WJ, Rama D, Pineda CA. 2001b. Elemental distribution in *Senecio anomalochrous*, a Ni hyperaccumulator from South Africa. *South African Journal of Science* **97**: 593–595.

Montargès-Pelletier E, Chardot V, Echevarria G, Michot LJ, Bauer A, Morel J-L. 2008. Identification of nickel chelators in three hyperaccumulating plants: an X-ray spectroscopic study. *Phytochemistry* **69**: 1695–1709.

Pollard AJ, Reeves RD, Baker AJM. 2014. Facultative hyperaccumulation of heavy metals and metalloids. *Plant Science* **217–218**: 8–17.

Proctor J. 2003. Vegetation and soil and plant chemistry on ultramafic rocks in the tropical Far East. *Perspectives in Plant Ecology Evolution and Systematics* **6**: 105–124.

Prozesky VM, Przybylowicz WJ, van Achterbergh E, Churms CL, Pineda CA, Springhorn KA, Pilcher JV, Ryan CG, Kritzinger J, Schmitt H *et al.* 1995. The NAC nuclear microprobe facility. *Nuclear Instruments and Methods in Physics Research B* **104**: 36–42.

Przybyłowicz W, Mesjasz-Przybyłowicz J, Migula P, Nakonieczny M, Augustyniak M, Tarnawska M, Turnau K, Ryszka P, Orłowska E, Zubek Sz *et al.* 2005. Micro-PIXE in ecophysiology. *X-Ray Spectrometry* **34**: 285–289.

Przybyłowicz W, Mesjasz-Przybyłowicz J, Pineda C, Churms C, Springhorn K, Prozesky V. 1999. Biological applications of the NAC nuclear microprobe. *X Ray Spectrometry* **28**: 237–243.

Przybylowicz WJ, Pineda CA, Prozesky VM, Mesjasz-Przybylowicz J. 1995. Investigation of Ni hyperaccumulation by true elemental imaging. *Nuclear Instruments and Methods in Physics Research B* **104**: 176–181.

Reeves RD. 2003. Tropical hyperaccumulators of metals and their potential for phytoextraction. *Plant and Soil* **249**: 57–65.

Robinson BH, Lombi E, Zhao FJ, McGrath SP. 2003. Uptake and distribution of nickel and other metals in the hyperaccumulator *Berkheya coddii*. *New Phytologist* **158**: 279–285.

Ryan C. 2000. Quantitative trace element imaging using PIXE and the nuclear microprobe. *International Journal of Imaging Systems and Technology* **11**: 219–230.

Ryan C, Cousens D, Sie S, Griffin W. 1990a. Quantitative Analysis of PIXE spectra in geoscience applications. *Nuclear Instruments and Methods in Physics Research B* **49**: 271–276.

Ryan C, Cousens D, Sie S, Griffin W, Suter G, Clayton E. 1990b. Quantitative PIXE micro analysis of geological material using the CSIRO proton microprobe. *Nuclear Instruments and Methods in Physics Research B* **47**: 55–71.

Ryan C, Jamieson D. 1993. Dynamic analysis: on-line quantitative PIXE microanalysis and its use in overlap-resolved elemental mapping. *Nuclear Instruments and Methods in Physics Research B* **77**: 203–214.

Ryan C, Jamieson D, Churms C, Pilcher J. 1995. A new method for on-line true-elemental imaging using PIXE and the proton microprobe. *Nuclear Instruments and Methods in Physics Research B* **104**: 157–165.

Schaumlöffel D, Ouerdane L, Bouyssiere B, Łobiński R. 2003. Speciation analysis of nickel in the latex of a hyperaccumulating tree *Sebertia acuminata* by HPLC and CZE with ICP MS and electrospray MS-MS detection. *Journal of Analytical Atomic Spectrometry* **18**: 120–127.

Severne BC. 1974. Nickel accumulation by *Hybanthus floribundus*. *Nature* **248**: 807–808.

Spurr AR. 1969. A low-viscosity epoxy resin embedding medium for electron microscopy. *Journal of Ultrastructure Research* **26**: 31–43.

Swenson U, Munzinger J. 2010. Revision of *Pycnandra* subgenus *Sebertia* (Sapotaceae) and a generic key to the family in New Caledonia. *Adansonia, sér. 3* **32**: 239–249.

Tappero R, Peltier E, Gräfe M, Heidel K, Ginder-Vogel M, Livi KJT, Rivers ML, Marcus MA, Chaney RL, Sparks DL. 2007. Hyperaccumulator *Alyssum murale* relies on a different metal storage mechanism for cobalt than for nickel. *New Phytologist* **175**: 641–654.

Tylko G, Mesjasz-Przybyłowicz J, Przybyłowicz WJ. 2007. X-ray microanalysis of biological material in the frozen-hydrated state by PIXE. *Microscopy Research and Technique* **70**: 55–68.